



Real-Time Tropospheric Delay Estimation Using GPS/Galileo Observations and NAVCAST Products

Mohamed Abdelazeem ⁽¹⁾, Ahmed El-Rabbany ⁽²⁾

(1) Civil Engineering Department, Aswan University, Egypt

(2) Civil Engineering Department, Ryerson University, Canada

Abstract

Precise estimation of real-time zenith tropospheric delay (RT-ZTD) is critical for real-time atmospheric sounding applications. Recently, the NAVCAST real-time service has been launched, which provides GPS/Galileo precise satellite orbit and clock corrections. This study aims to assess the precision of real-time zenith tropospheric delay obtained through the real-time GPS/Galileo precise point positioning (RT-PPP) solution. GPS/Galileo observations, spanning three successive days, from a number of globally-distributed reference stations are first acquired and processed in the real-time mode using the NAVCAST real-time products. The RT-ZTD is then estimated and compared with the center for orbit determination in Europe (CODE) rapid tropospheric product counterpart. It is shown that the RT-ZTD estimates are in good agreement with the CODE counterparts with a maximum standard deviation (STD) of 22.2 mm. The addition of Galileo observations improves the precision of the RT-ZTD estimates by about 25% in comparison with the GPS-only solution.

1. Introduction

Zenith tropospheric delay (ZTD) is a key parameter for precise positioning, weather forecasts and climate change applications. ZTD can be estimated using various techniques, including global navigation satellite systems (GNSS), radiosonde, and very long baseline interferometry (VLBI) techniques. In comparison with traditional techniques, GNSS-PPP represents a cost-effective precise technique for ZTD determination with high-resolution. As such, the GNSS-derived ZTD has become an important approach for real-time atmospheric sounding applications, particularly with the recent increase in the number of GNSS satellites and the availability of real-time precise satellite orbit and clock correction services.

To achieve a reliable real-time PPP solution, the international GNSS service (IGS) has launched its freely available real-time service (IGS-RTS). The RTS provides real-time precise satellite orbit and clock corrections through a number of analysis centers [1]. Recently, Spaceop GmbH, which is the prime contractor responsible for Galileo operation, has launched a newly real-time satellite orbit and clock correction service for GPS and Galileo systems, namely NAVCAST [2]. The

positioning accuracy of the GPS/Galileo PPP solution using the NAVCAST products can reach centimeter-level in static mode and decimeter-level in kinematic mode [3].

Real-time zenith tropospheric delay estimation has been investigated by a number of researchers e.g., [4, 5, 6, 7, 8, 9, 10, 11, 12 and 13]. [8] evaluated the obtained RT-ZTD from multi-GNSS observations using different IGS-RTS product streams. The U.S. Naval Observatory (USNO) final troposphere product has been used as reference. It has been shown that the RT-ZTD values estimated from the GFZC2 products were better than those obtained through the IGS-RTS streams. In addition, the estimated RT-ZTD from multi-GNSS solution has been improved by about 22.2 % with respect to the GPS-only solution.

In this research, the precision of the estimated real-time zenith tropospheric delays from GPS/Galileo observations is assessed. The RT-ZTDs are obtained through the GPS-only and the GPS/Galileo real-time PPP solutions using the NAVCAST satellite orbit and clock corrections. GPS/Galileo observations from a number of global reference stations over three successive days are used. The obtained RT-ZTD is validated through comparison with the center for orbit determination in Europe (CODE) rapid tropospheric product counterpart. It is shown that the precision of the obtained RT-ZTD is comparable with the post-processed CODE counterpart.

2. ZTD Estimation Using GPS/Galileo PPP

The mathematical expression for the GPS/Galileo ionosphere-free (IF) dual-frequency PPP model can be written as follows [14]:

$$P_{3G} = \rho_r^G + cdt_{r,G} - cdt^G + T_r^G + \varepsilon_{G,p3} \quad (1)$$

$$\Phi_{3G} = \rho_r^G + cdt_{r,G} - cdt^G + T_r^G + \tilde{N}^G + \varepsilon_{G,\Phi3} \quad (2)$$

$$P_{3E} = \rho_r^E + cdt_{r,G} - cdt^E + T_r^E + ISB + \varepsilon_{E,p3} \quad (3)$$

$$\Phi_{3E} = \rho_r^E + cdt_{r,G} - cdt^E + T_r^E + \tilde{N}^E + ISB + \varepsilon_{E,\Phi3} \quad (4)$$

where G and E refer to the GPS and Galileo satellite systems, respectively; P_3 and Φ_3 represent the ionosphere-free linear combination of pseudorange and carrier phase observations, respectively; ρ_r^G and ρ_r^E are the satellite-receiver true geometric range; c is the speed of light in vacuum; $dt_{r,G}$ indicates to the sum of the GPS receiver clock error and the GPS IF receiver differential code bias;

dt^G and dt^E are the satellite clock error, which includes the IF satellite differential code bias; T_r^G and T_r^E are the tropospheric delay; \tilde{N}^G and \tilde{N}^E are the non-integer ambiguity term for phase observations, including the IF receiver differential code and phase biases, and the IF satellite differential code and phase biases; ISB is the inter-system bias, which is the difference in the IF receiver differential code bias between the GPS and Galileo satellite systems; ε_{p3} and $\varepsilon_{\phi3}$ are the code and phase un-modeled residual errors.

The tropospheric delay can be broken down mathematically into two components, the wet and the dry, as follows:

$$T_r^G = Z_h \times MF_h + Z_w \times MF_w \quad (5)$$

$$T_r^E = Z_h \times MF_h + Z_w \times MF_w \quad (6)$$

where Z_h and Z_w represent the zenith hydrostatic delay (ZHD) and the zenith wet delay (ZWD), respectively; MF_h and MF_w refer to the hydrostatic and the wet mapping functions, respectively. The ZHD can be accounted for using the Saastamoinen model [15], while the ZWD is estimated as a by-product of the PPP solution.

For parameter estimation, the state vector (\mathbf{X}) of the unknown parameters can be expressed as:

$$\mathbf{X} = (\Delta x \ \Delta y \ \Delta z \ cdt_{r,G} \ Z_w \ ISB \ \tilde{N})^T \quad (7)$$

where $\Delta x, \Delta y$ and Δz refer to the corrections to the approximate initial receiver coordinates.

3. GPS/Galileo Real-Time Data Sets

Our evaluation study has been carried out using GPS/Galileo observations from four globally distributed reference stations (Figure 1). The distribution of the reference stations has been chosen to represent different latitudes and heights (Table 1) in order to reflect the different tropospheric characteristics. GPS/Galileo observations over three consecutive days (i.e., day of year (DOY) 20, 21 and 22 in 2020) have been downloaded [16]. The days have been selected in order to examine the daily performance of the RT-ZTD estimates.

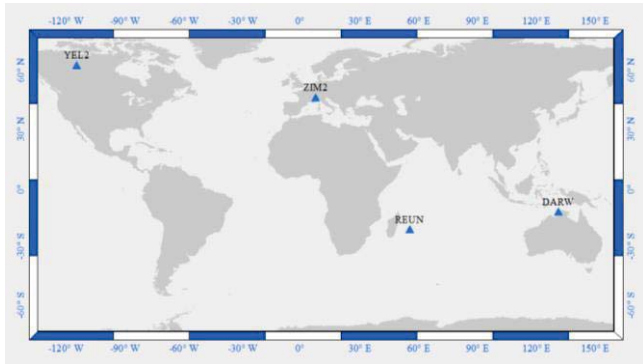


Figure 1. Examined station distributions

Table 1. Approximate coordinates of examined stations

Station	Longitude	Latitude	Height (m)
YEL2	-114.481°	62.481°	181.0
ZIM2	7.090°	46.155°	956.50
REUN	55.099°	-21.042°	1558.4
DARW	131.036°	-12.149°	125.2

The NAVCAST service provides the real-time satellite orbit and clock corrections every 5 seconds in different streams [2]. In our study, the CLKA0_DEU stream has been used, which includes orbit and clock corrections. The real-time NAVCAST corrections has been obtained through the networked transport of RTCM via internet protocol (NTRIP) using the BKG NTRIP client (BNC) software [17].

Each observation file has a 24-hour time window and 30-second time interval. To estimate the RT-ZTD in real-time mode, the pre-saved NAVCAST orbit and clock corrections, the broadcast ephemerides (i.e., BRDM) available from [18], and the observation files have been used in the BNC software in order to obtain the PPP solution. The elevation angle has been selected to be 10°. The RT-ZTD values have been estimated every 5 minutes.

Figure 2 illustrates the average of the number of tracked satellites and the position dilution of precision (PDOP) values at the examined stations. It is noticed that the addition of Galileo constellation increases the number of the visible satellites and enhances the PDOP values.

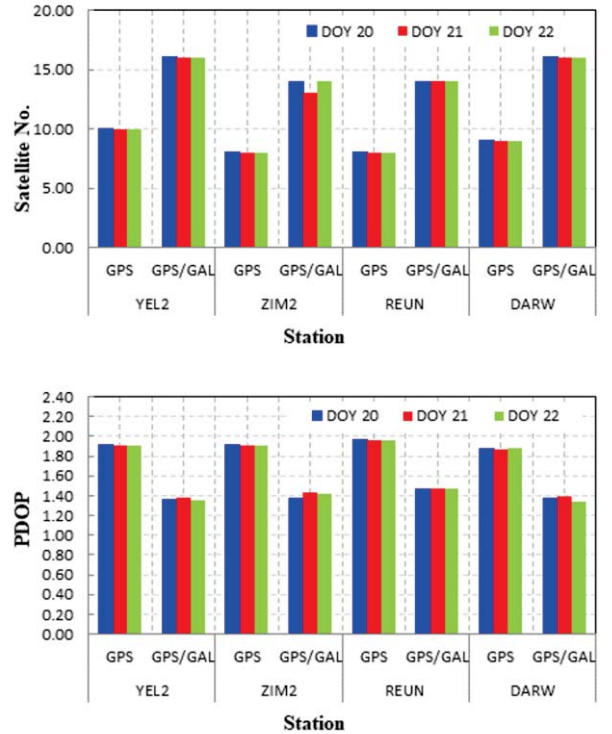


Figure 2. Number of visible satellites (up) and PDOP values (down) over the examined stations

4. Results and Analysis

To estimate the real-time ZTD, the GPS/Galileo observations collected at the reference stations are processed using the BNC software in the real-time PPP mode. Two different PPP scenarios are executed, namely the GPS-only and GPS/Galileo solutions. Subsequently, the RT-ZTD estimates, which are obtained as by-products of the PPP solutions, are compared with CODE's rapid tropospheric counterparts [19]. Figure 3 shows the RT-ZTD time series for the examined stations over three days. It can be seen that the estimated RT-ZTD values from both of the GPS-only and GPS/Galileo solutions closely match those of the CODE counterparts.

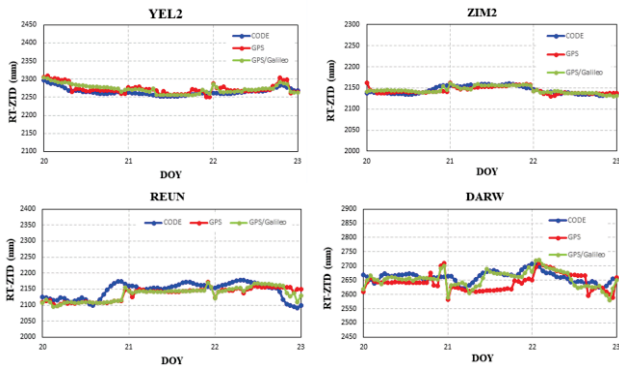


Figure 3. RT-ZTD estimates over the examined stations

To validate the estimated RT-ZTD with respect to the CODE counterparts, the standard deviations (STD) for the differences are computed for the examined days, which are presented in Table 2. It should be mentioned that the STDs of the CODE ZTD are less than 1 mm over our examined stations [19].

Table 2. STD for the RT-ZTD differences in mm

Station	solution	DOY	DOY	DOY
		20	21	22
YEL2	GPS	7.8	8.0	9.1
	GPS/GAL	5.3	5.0	6.5
ZIM2	GPS	9.3	6.0	3.4
	GPS/GAL	10.3	4.5	2.6
REUN	GPS	20.1	10.9	28.5
	GPS/GAL	20.6	9.4	23.4
DARW	GPS	23.7	34.8	27.7
	GPS/GAL	18.4	20.1	25.6

As can be seen in Table 2, the estimated RT-ZTD values agree at the mm-cm level with the CODE counterparts. An exception is for station DARW, which is located at a low latitude. This might be attributed to a relatively lower model performance at low latitudes. In addition, the STDs of the estimated RT-ZTD at station REUN are slightly larger than those of YEL2 and ZIM2 counterparts, which might be attributed to the much higher altitude of station REUN.

To further verify the precision of the estimated RT-ZTD with respect to the CODE counterpart, the distribution of the RT-ZTD-CODE differences is determined, which is depicted in Figure 4.

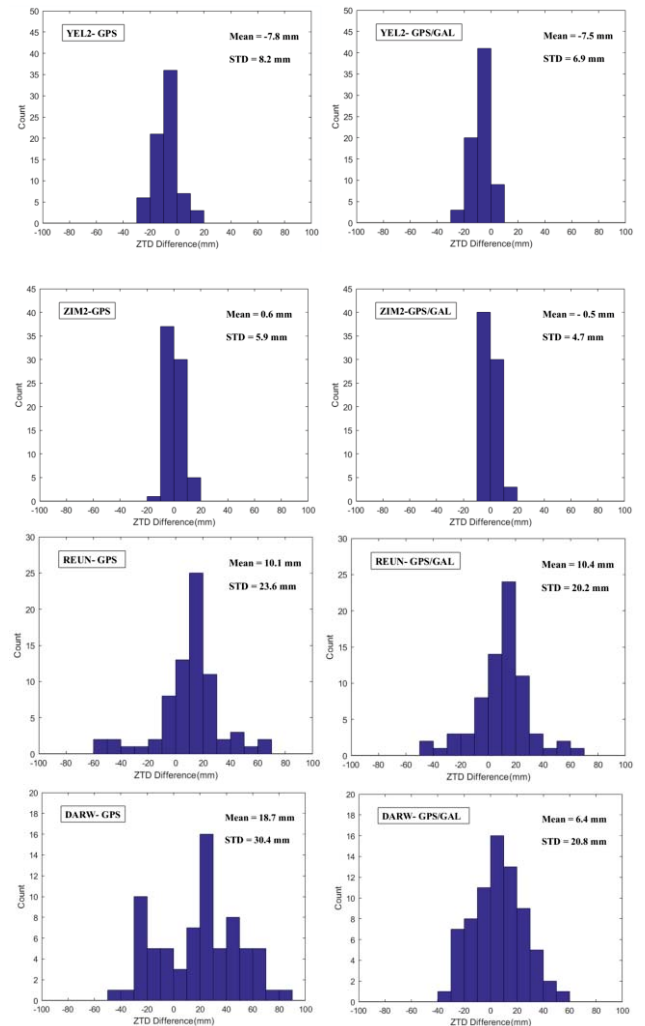


Figure 4. Distribution of the RT-ZTD differences over the examined stations.

It is shown that the precision of the estimated RT-ZTD from the GPS/Galileo solution is better than the one obtained from the GPS-only solution. As an example, the RT-ZTD precision at station YEL2 is improved from 8.2 to 6.9 mm. For station ZIM2, the RT-ZTD precision is enhanced from 5.9 to 4.7 mm. The precision of the estimated RT-ZTD is also improved from 23.6 to 20.2 mm and from 30.4 to 20.8 mm for stations REUN and DARW, respectively. This is expected, as the satellite geometry is improved through the addition of Galileo constellation.

Additionally, the statistical parameters including the mean, minimum, maximum and STD values are computed and summarized in Table 3 in order to assess the overall precision of the obtained RT-ZTDs. It is clear that the precision of the RT-ZTD obtained through the GPS/Galileo PPP solution is better than that of the GPS-only PPP solution. On average, the precision of the estimated RT-

ZTD from the GPS/Galileo solution is improved by about 25% in comparison with the GPS-only solution.

Table 3. Statistical parameters for the RT-ZTD difference

Parameter (mm)	GPS-only	GPS/Galileo
Mean	5.4	2.2
Min.	81.6	75.5
Max.	-58.8	-43.1
STD	22.2	16.5

5. Conclusion

This study assesses the precision of the real-time ZTD obtained through the GPS/Galileo PPP using the NAVCAST orbit and satellite corrections. GPS/Galileo observations from a number of globally distributed reference stations spanning three successive days have been processed using the BNC software in order to assess the daily performance of the RT-ZTD model. The RT-ZTD has been obtained through the GPS-only and the GPS/Galileo PPP solutions. The estimated RT-ZTD have been validated with respect to the CODE rapid tropospheric products. It has been shown that the estimated RT-ZTD values agree with the CODE counterparts with a maximum standard deviation of 22.2 mm. In addition, the precision of the RT-ZTD obtained through the GPS/Galileo PPP solution is improved by about 25% in comparison with the GPS-only counterpart. The obtained RT-ZTD can be used in real-time atmospheric sounding applications, including nowcasting and forecasting weather applications.

6. References

- [1] IGS Real-Time Pilot Project, http://www.rtigs.net/pilot/rtpc_ACs.php. Accessed on January 20th, 2020.
- [2] Spaceopal, <https://spaceopal.com/navcast/>. Accessed on January 20th, 2020.
- [3] A. Elmezayen and A. El-Rabbany, "Real-Time GPS/Galileo Precise Point Positioning Using NAVCAST Real-Time Corrections," *Positioning*, vol. 10, pp. 35-49, 2019.
- [4] F. Ahmed, P. Václavovic, F. N. Teferle, J. Douša, R. Bingley, and D. Laurichesse, "Comparative analysis of real-time precise point positioning zenith total delay estimates," *GPS Solutions*, vol. 20, pp. 187-199, 2014.
- [5] W. Ding, F. N. Teferle, K. Kazmierski, D. Laurichesse, and Y. Yuan, "An evaluation of real-time troposphere estimation based on GNSS Precise Point Positioning," *Journal of Geophysical Research: Atmospheres*, vol. 122, pp. 2779-2790, 2017.
- [6] X. Li, F. Zus, C. Lu, G. Dick, T. Ning, M. Ge, *et al.*, "Retrieving of atmospheric parameters from multi-GNSS in real time: Validation with water vapor radiometer and numerical weather model," *Journal of Geophysical Research: Atmospheres*, vol. 120, pp. 7189-7204, 2015.
- [7] Y. Lou, J. Huang, W. Zhang, H. Liang, F. Zheng, and J. Liu, "A New Zenith Tropospheric Delay Grid Product for Real-Time PPP Applications over China," *Sensors (Basel)*, vol. 18, Dec 27 2017.
- [8] C. Lu, X. Chen, G. Liu, G. Dick, J. Wickert, X. Jiang, *et al.*, "Real-Time Tropospheric Delays Retrieved from Multi-GNSS Observations and IGS Real-Time Product Streams," *Remote Sensing*, vol. 9, p. 1317, 2017.
- [9] L. Pan and F. Guo, "Real-time tropospheric delay retrieval with GPS, GLONASS, Galileo and BDS data," *Sci Rep*, vol. 8, p. 17067, Nov 20 2018.
- [10] X. Yang, G. Chang, Q. Wang, S. Zhang, Y. Mao, and X. Chen, "An adaptive Kalman filter based on variance component estimation for a real-time ZTD solution," *Acta Geodaetica et Geophysica*, vol. 54, pp. 89-121, 2019.
- [11] Y. Yao, X. Xu, C. Xu, W. Peng, and Y. Wan, "Establishment of a Real-Time Local Tropospheric Fusion Model," *Remote Sensing*, vol. 11, p. 1321, 2019.
- [12] Y. Yuan, L. Holden, A. Kealy, S. Choy, and P. Hordyniec, "Assessment of forecast Vienna Mapping Function 1 for real-time tropospheric delay modeling in GNSS," *Journal of Geodesy*, vol. 93, pp. 1501-1514, 2019.
- [13] Q. Zhao, Y. Yao, W. Yao, and Z. Li, "Real-time precise point positioning-based zenith tropospheric delay for precipitation forecasting," *Sci Rep*, vol. 8, p. 7939, May 21 2018.
- [14] B. Hofmann-Wellenhof, H. Lichtenegger and E. Walse, "GNSS Global Navigation Satellite Systems: GPS, GLONASS, Galileo, and More," Springer, New York, 2008.
- [15] J. Saastamoinen, "Contributions to the theory of atmospheric refraction," *Bulletin Géodésique*, 105, 279-298, 1972.
- [16] IGS, International GNSS Service, <ftp://cddis.gsfc.nasa.gov/gnss/data/daily/>. Accessed on January 20th, 2020.
- [17] BKG BNC software, <https://igs.bkg.bund.de/ntrip/bnc>. Accessed on January 20th, 2020.
- [18] Broadcast Ephemerides (BRDM), <ftp://cddis.gsfc.nasa.gov/gnss/data/campaign/mgex/daily/rinex3/2020/brdm/>. Accessed on January 20th, 2020.
- [19] CODE, Center for Orbit Determination in Europe, <ftp://ftp.aiub.unibe.ch/CODE/>. Accessed on January 20th, 2020.